

# Predicting a Two-dimensional P<sub>2</sub>S<sub>3</sub> Monolayer: A Global Minimum Structure

Hang Xiao<sup>[a]</sup>, Xiaoyang Shi<sup>[a]</sup>, Feng Hao<sup>[a]</sup>, Xiangbiao Liao<sup>[a]</sup>, Yayun Zhang<sup>[a,c]</sup> and Xi  
Chen<sup>\*[a,b]</sup>

[a] Columbia Nanomechanics Research Center, Department of Earth and Environmental  
Engineering, Columbia University, New York, NY 10027, USA, E-mail: xichen@columbia.edu

[b] SV Laboratory, School of Aerospace, Xi'an Jiaotong University, Xi'an 710049, China

[c] College of Power Engineering, Chongqing University, Chongqing 400030, China

**Abstract:** Based on extensive evolutionary algorithm driven structural search, we propose a new diphosphorus trisulfide (P<sub>2</sub>S<sub>3</sub>) 2D crystal, which is dynamically, thermally and chemically stable as confirmed by the computed phonon spectrum and *ab initio* molecular dynamics simulations. This 2D crystalline phase of P<sub>2</sub>S<sub>3</sub> corresponds to the global minimum in the Born-Oppenheimer surface of the phosphorus sulfide monolayers with 2:3 stoichiometries. It is a wide band gap (4.55 eV) semiconductor with P-S  $\sigma$  bonds. The electronic properties of P<sub>2</sub>S<sub>3</sub> structure can be modulated by stacking into multilayer P<sub>2</sub>S<sub>3</sub> structures, forming P<sub>2</sub>S<sub>3</sub> nanoribbons or rolling into P<sub>2</sub>S<sub>3</sub> nanotubes, expanding its potential applications for the emerging field of 2D electronics.

**Keywords:** Semiconductors • 2D Crystal • Diphosphorus trisulfide • Wide band gap • Global minimum structure

**Text:**

The epic discovery of graphene [1], a two-dimensional (2D) phase of carbon, has paved the way for the synthesis of many other 2D materials, including the 2D insulator boron nitride (BN) [2–4], graphene-like group IV 2D materials, i.e. semimetallic silicene, germanene, and stanine [5–11], 2D transition-metal dichalcogenides [12–16], such as molybdenum disulfide [2,17,18] and tungsten disulfide [19], and recently, 2D phosphorus, i.e. phosphorene [20], which holds great promise for applications in electronics and optoelectronics.

The reduced dimensionality and symmetry of 2D materials, lead to unique electronic, optical and mechanical properties that differ from their bulk counterparts [21,22], offering possibilities for numerous advanced applications. For instance, transistors made with single layer MoS<sub>2</sub> present room-temperature current on/off ratios of 10<sup>8</sup> [18]. Two-dimensional materials also offer novel opportunities for fundamental studies of unique physical and chemical phenomena in 2D systems [23,24]. More interestingly, stacking different 2D crystals into heterostructures (often referred to as ‘van der Waals’) have recently been achieved and investigated, revealing new phenomena and novel properties [25].

Over the past decade, a number of experimental methods have been developed to produce monolayer nanosheets by exfoliating layered materials with oxidation, ion

intercalation/exchange, or surface passivation induced by solvents [26,27]. Theoretical methods have been employed to search new two-dimensional materials such as evolutionary crystal structure search [28–30] and particle swarm optimization (PSO) [31]. For example, a novel 2D Be<sub>2</sub>C monolayer, with each carbon atom binding to six Be atoms to form a quasi-planar hexacoordinate carbon moiety, was discovered by Li *et al* [32]. And in our previous work [33], we discovered a novel light-emitting 2D crystal with a wide direct band gap, namely S<sub>3</sub>N<sub>2</sub> monolayer, using the evolutionary crystal structure search method. The amazing properties of the S<sub>3</sub>N<sub>2</sub> 2D crystal inspired us to explore the possibility of other group V-VI 2D crystals.

In this work, we proposed a new two-dimensional crystal, diphosphorus trisulfide (P<sub>2</sub>S<sub>3</sub>) with 3 polymorphs:  $\alpha$ -P<sub>2</sub>S<sub>3</sub> (Fig. 1(a)),  $\beta$ -P<sub>2</sub>S<sub>3</sub> (Fig. 1(b)) and  $\gamma$ -P<sub>2</sub>S<sub>3</sub> (Fig. 1(c)). The ground state structure of these polymorphs were obtained using the evolutionary algorithm driven structural search code USPEX [28–30]. These P<sub>2</sub>S<sub>3</sub> polymorphs were further geometry optimized with density functional calculations with Perdew–Burke–Ernzerhof (PBE) [34] exchange-correlation functional using the Cambridge series of total-energy package (CASTEP) [35,36]. A plane-wave cutoff energy of 700 eV was used, and Monkhorst-Pack [37] meshes with 0.02 Å<sup>-1</sup>  $k$ -point spacing were adopted. The convergence test of cutoff energy and  $k$ -point mesh was conducted. In calculating the binding energy of bilayer  $\alpha$ -P<sub>2</sub>S<sub>3</sub>, the empirical dispersion correction schemes proposed by Grimme (D2) [38] was used in combination with PBE functional to properly describe the van der Waals (vdW) interactions between  $\alpha$ -P<sub>2</sub>S<sub>3</sub> layers. Since the band gaps may be dramatically underestimated by the GGA level DFT [39,40], the quasiparticle GW calculation [41] of the band structure was carried out using YAMBO software package [42]. The Green function and Coulomb screening were constructed from the PBE results obtained by Quantum Espresso [43], and the plasmon-pole model was used for computing the screening. The G<sub>0</sub>W<sub>0</sub>

approximation was adopted in carrying out the GW approximation, since it gives very good results for many materials without  $d$  electrons [44]. All structure optimizations were conducted without imposing any symmetry constraints. The conjugate gradient method (CG) was used to optimize the atomic positions until the change in total energy was less than  $5 \times 10^{-6}$  eV/atom, maximum stress within 0.01 GPa and the maximum displacement of atoms was less than  $5 \times 10^{-5}$  Å.

The fully relaxed  $P_2S_3$  polymorphs are depicted in Fig. 1. These  $P_2S_3$  polymorphs are 2D covalent networks composed solely of  $\sigma$  bonds (bonding is depicted by isosurfaces of the electron density). For  $\alpha$ - $P_2S_3$  (space group Pmn21), the unit cell (see Fig. 1(a)) consists of ten atoms with lattice constants  $a = 4.71$  Å,  $b = 10.62$  Å, P-S bonds with bond lengths  $d_1 = 2.14$  Å,  $d_2 = 2.12$  Å,  $d_3 = 2.15$  Å, and bond angles  $\theta_1 = 103.8^\circ$ ,  $\theta_2 = 105.7^\circ$ ,  $\theta_3 = 96.2^\circ$ ,  $\theta_4 = 94.4^\circ$  and  $\theta_5 = 107.4^\circ$ . The unit cell of  $\beta$ - $P_2S_3$  (space group Cmm2) consists of five atoms with lattice constants  $a_1 = a_2 = 5.35$  Å, the angle between unit vector  $a_1$  and  $a_2$ ,  $\gamma = 108.8^\circ$ , P-S bonds with bond lengths  $d_1 = 2.14$  Å,  $d_2 = 2.15$  Å, and bond angles  $\theta_1 = 93.0^\circ$ ,  $\theta_2 = 111.4^\circ$ ,  $\theta_3 = 132.4^\circ$  and  $\theta_4 = 94.1^\circ$  (see Fig. 1(b)). The unit cell of  $\gamma$ - $P_2S_3$  (space group P31m) consists of five atoms with lattice constants  $a_1 = a_2 = 5.92$  Å, P-S bonds with bond length  $d_1 = 2.16$  Å, and bond angles  $\theta_1 = 95.1^\circ$  and  $\theta_2 = 104.9^\circ$  (see Fig. 1(c)). For these polymorphs, the Brillouin zones with the relevant high-symmetry k-points are depicted in the inset figures in Fig. 1. The cohesive energies of  $\alpha$ - $P_2S_3$ ,  $\beta$ - $P_2S_3$  and  $\gamma$ - $P_2S_3$  are -3.64 eV, -3.59 eV and -3.60 eV, so the most energetically stable polymorph is  $\alpha$ - $P_2S_3$ .

Even if the structure optimizations using CG method indicate the stability of these free standing  $P_2S_3$  polymorphs, further tests should be conducted to assure these polymorphs are stable in the local minimum and can remain stable above the room temperature. First, by

conducting phonon dispersion calculation of the free-standing  $P_2S_3$  polymorphs, we verified that all phonon frequencies of  $\alpha$ - $P_2S_3$  are real (Fig. 2(a)), confirming the dynamic stability of this structure. However,  $\beta$ - $P_2S_3$  and  $\gamma$ - $P_2S_3$  are not dynamically stable, since they have imaginary phonon frequencies (Fig. 2(b-c)). Thus, our focus will be on the properties of the dynamically stable  $\alpha$ - $P_2S_3$  in the following discussions.

For  $\alpha$ - $P_2S_3$ , the enthalpy of formation  $\Delta H$  from the elements



calculated by CASTEP at  $T=0$  K is -14.2 kcal/mol. This means  $\alpha$ - $P_2S_3$  is an energetically favorable composition relative to phosphorus and sulfur in their solid state.

To verify the stability of the structure under high temperatures, *ab initio* molecular dynamics (MD) simulations (shown in Fig. 3) were performed at the PBE [34] /GTH-DZVP [45] level in the NPT ensemble with the CP2K [46] code. The simulations were run for 10 ps under ambient pressure under temperature  $T= 1000$  K and no breaking of the bonds was seen, indicating a high degree of stability. To further verify the chemical stability of the structure in air, *ab initio* MD of  $\alpha$ - $P_2S_3$  crystal exposed to very high pressure gases ( $O_2$ ,  $N_2$ ,  $H_2O$  and  $H_2$ ) at temperatures  $T= 1000$  K were conducted (Fig. 4). In our MD simulations, the number density of gas molecules was  $57.5 \times 10^{25} \text{ m}^{-3}$ . Such high gas pressure were also used to study oxidation of graphene [47] and phosphorene [48] with MD simulations.  $\alpha$ - $P_2S_3$  structure remains intact under these very high gas pressure for 10 ps (Fig. 4), indicating its chemical stability in air above the room temperature.

The quasiparticle and DFT band structures and density of states of the 2D  $\alpha$ - $P_2S_3$  crystal are shown in Fig. 5. Calculations carried out using GW method showed that the  $\alpha$ - $P_2S_3$  structure

is a semiconductor with a wide band gap of 4.55 eV (calculations carried out using PBE functional underestimate the band gap by 2.05 eV). The valence band maximum (VBM) is composed of mainly the orbitals of sulfur atoms, while the conduction band minimum (CBM) is more or less evenly contributed by the orbitals of phosphorus and sulfur atoms (see Fig. 5).

Our analysis shows that not only single-layer  $\alpha$ -P<sub>2</sub>S<sub>3</sub>, but also bilayer and its 3D phase constructed by the stacking of  $\alpha$ -P<sub>2</sub>S<sub>3</sub> monolayers, are stable. The minimum energy stacking for the bilayer and 3D phase are shown in inset figures in Fig. 5. The binding energy between layers is weak and is only 0.13 J/m<sup>2</sup>, which is predominantly vdW attraction energy. The DFT band gaps are reduced by 0.14 eV by just stacking P<sub>2</sub>S<sub>3</sub> into a bilayer. By stacking P<sub>2</sub>S<sub>3</sub> into 3D P<sub>2</sub>S<sub>3</sub> crystal, the DFT band gap is further reduced to 2.18 eV. Beside stacking, the electronic properties of P<sub>2</sub>S<sub>3</sub> can be modulated by cutting into P<sub>2</sub>S<sub>3</sub> nanoribbons or rolling up to form P<sub>2</sub>S<sub>3</sub> nanotubes, expanding its potential applications in 2D electronics.

In conclusion, we predicted a novel two-dimensional trisulfur dinitride (P<sub>2</sub>S<sub>3</sub>) crystal with high thermal stability using *ab initio* simulations. Band structures calculated using the GW method indicate that 2D P<sub>2</sub>S<sub>3</sub> crystal is a semiconductor with wide band gap of 4.55 eV. The P<sub>2</sub>S<sub>3</sub> solid is the first 2D crystal composed of phosphorus and sulfur, which also forms stable bilayer, 3D layered solid and nanoribbon structures. These structures with tunable band structures shed light on the applications for the emerging field of 2D electronics.

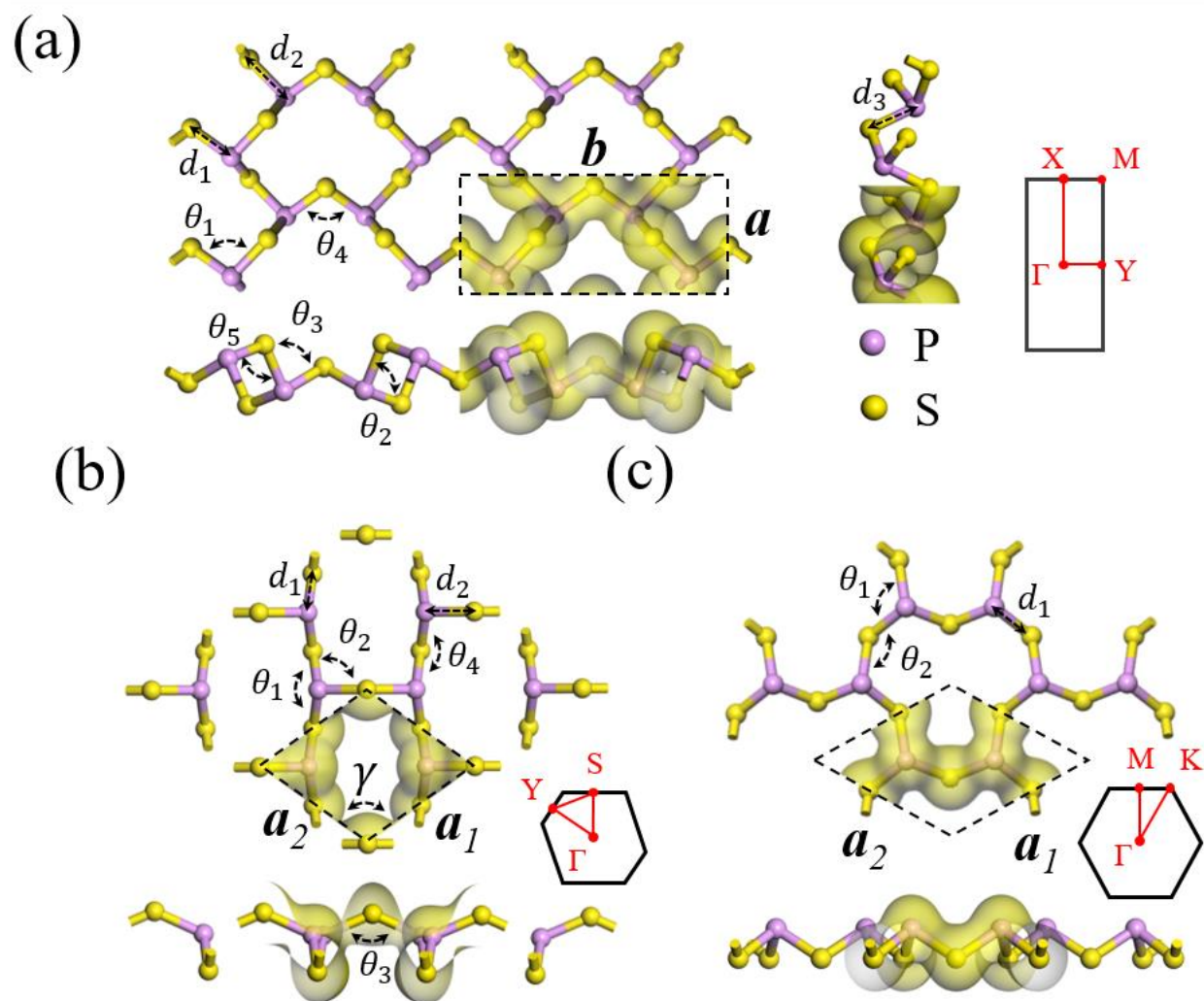


**Fig. 1.** 2D crystalline structures of  $\alpha$ - $\text{P}_2\text{S}_3$  (a),  $\beta$ - $\text{P}_2\text{S}_3$  (b) and  $\gamma$ - $\text{P}_2\text{S}_3$  (c). The Brillouin zone of each polymorph, with the relevant high-symmetry  $k$ -points indicated, is depicted in the inset figure. Bonding is depicted by an isosurface of the electron density.

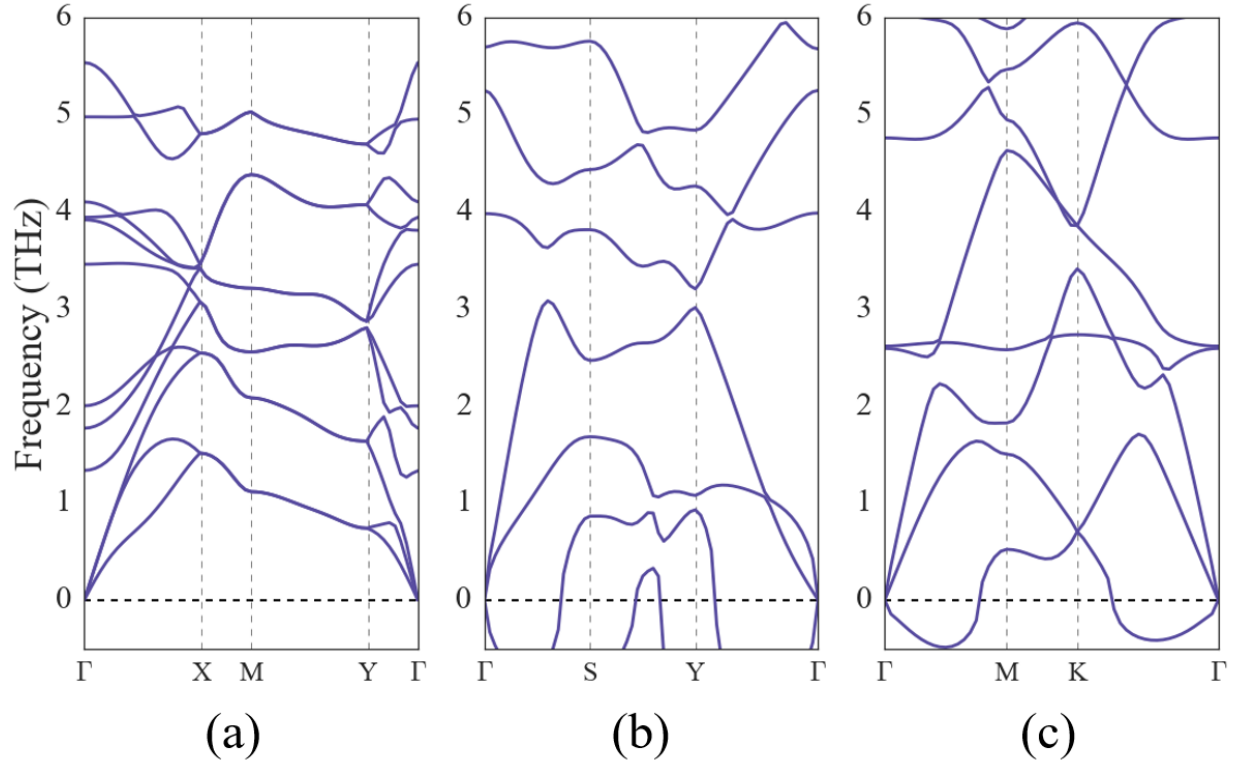


**Fig. 2.** The phonon dispersion relations of  $\alpha$ -P<sub>2</sub>S<sub>3</sub> (a),  $\beta$ -P<sub>2</sub>S<sub>3</sub> (b) and  $\gamma$ -P<sub>2</sub>S<sub>3</sub> (c). Dynamic stability of  $\alpha$ -P<sub>2</sub>S<sub>3</sub> is indicated by the absence of negative frequencies. However,  $\beta$ -P<sub>2</sub>S<sub>3</sub> and  $\gamma$ -P<sub>2</sub>S<sub>3</sub> are dynamically unstable, due to the presence of imaginary phonon frequencies.



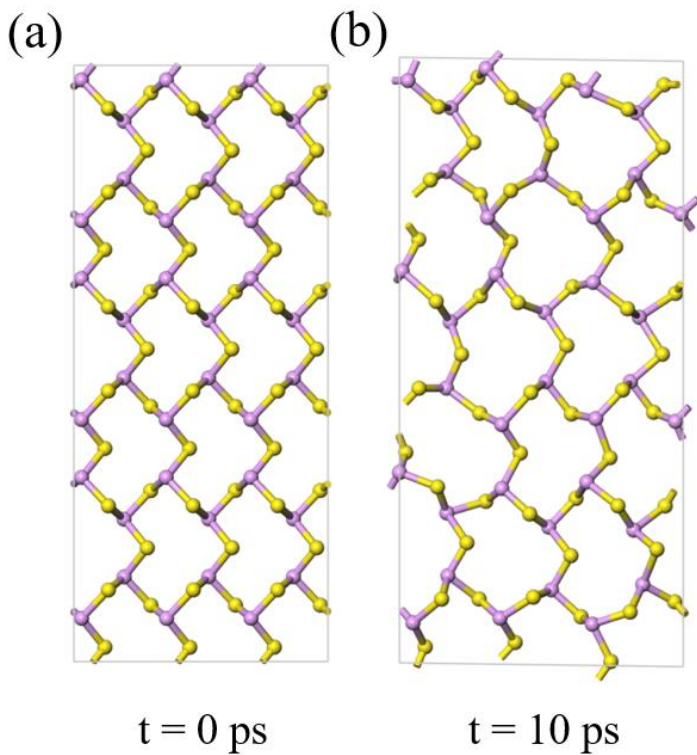


**Fig. 3.** *Ab initio* MD snapshots of the  $\alpha$ -P<sub>2</sub>S<sub>3</sub> supercell structures at temperature T = 1000 K under ambient pressure at time t = 0 ps (a) and t = 10 ps (b). No breaking of the bonds was seen during the 10 ps *ab initio* MD simulation, indicating a high degree of thermal stability.

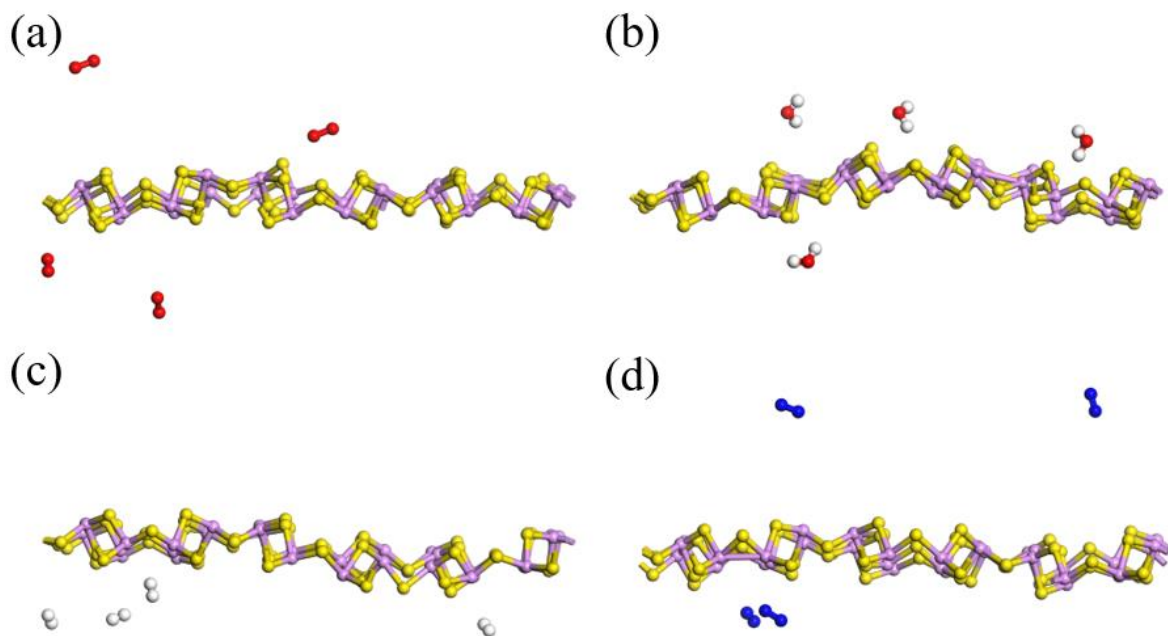


**Fig. 3.** *Ab initio* MD snapshots of the  $\alpha$ -P<sub>2</sub>S<sub>3</sub> supercell structures exposed to the high pressure oxygen gas (a), water vapour (b), hydrogen gas (c), and nitrogen gas (d) at temperatures  $T = 1000$  K. P<sub>2</sub>S<sub>3</sub> structures remain chemically stable during these 10 ps simulations, confirming the chemical stability of  $\alpha$ -P<sub>2</sub>S<sub>3</sub>.

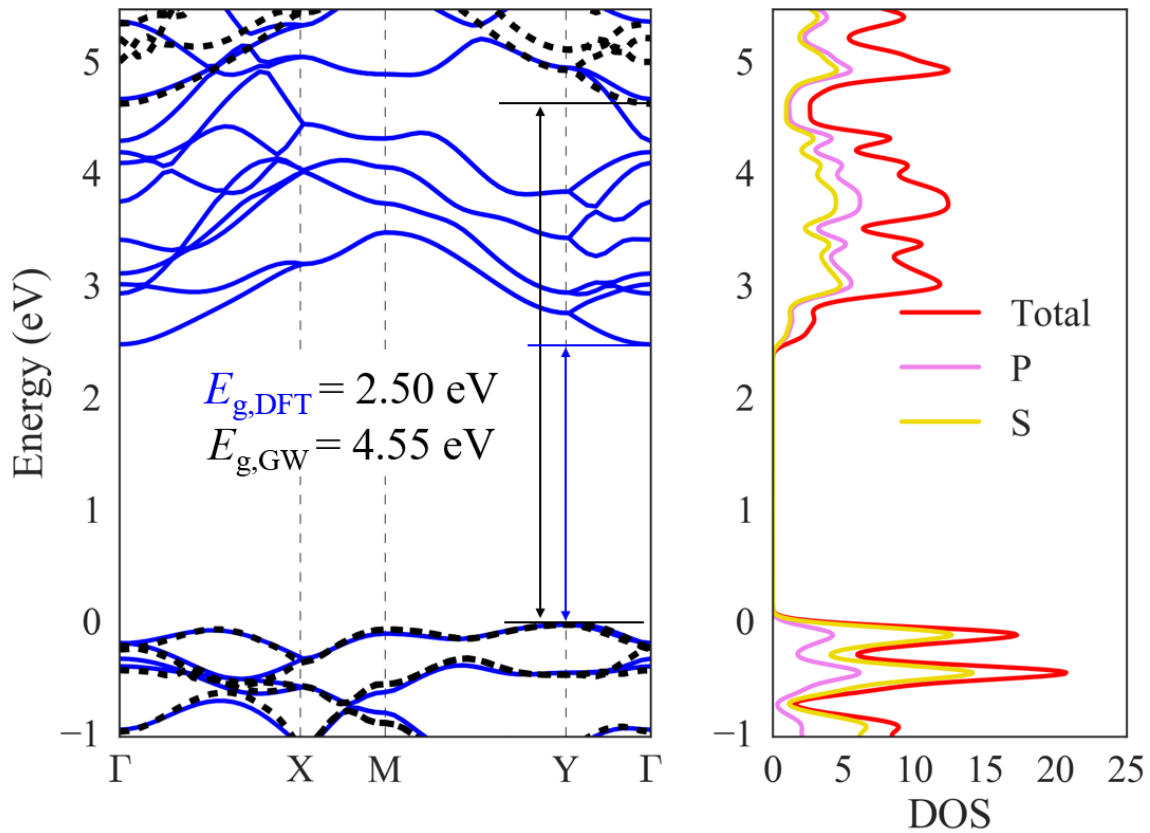


**Fig. 4.** Calculated band structure (left) obtained with the PBE functional (blue lines) and the GW method (black dash lines) for the  $\alpha$ -P<sub>2</sub>S<sub>3</sub> solid. The DOS (right) is obtained with the PBE functional.  $\alpha$ -P<sub>2</sub>S<sub>3</sub> crystal is a semiconductor with a wide band gap of 4.55 eV. The valence band maximum (VBM) is composed of mainly the orbitals of sulfur atoms, while the conduction band minimum (CBM) is more or less evenly contributed by the orbitals of phosphorus and sulfur atoms.

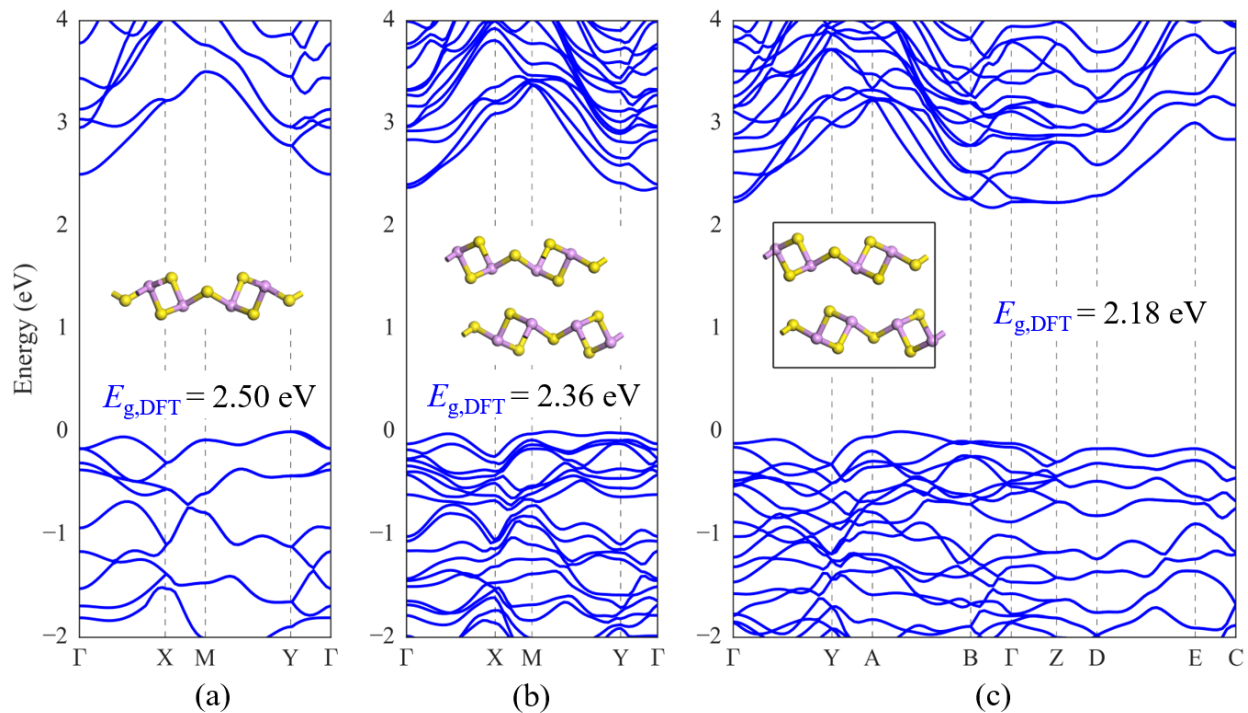


**Fig. 5.** The electronic band structures of the  $\alpha$ -P<sub>2</sub>S<sub>3</sub> monolayer (a),  $\alpha$ -P<sub>2</sub>S<sub>3</sub> bilayer (b) and  $\alpha$ -P<sub>2</sub>S<sub>3</sub> 3D crystal, obtained with the PBE functional. Monolayer, bilayer and 3D crystal structures of  $\alpha$ -P<sub>2</sub>S<sub>3</sub> are shown in inset figures.

## AUTHOR INFORMATION

### Corresponding Author

Xi Chen, E-mail: xichen@columbia.edu

### Author Contributions

These authors contributed equally.

### Notes

The authors declare no competing financial interests.

## ACKNOWLEDGMENT

The authors acknowledge the support from the National Natural Science Foundation of China (11372241 and 11572238), ARPA-E (DE-AR0000396) and AFOSR (FA9550-12-1-0159).

## REFERENCES

- [1] Novoselov K S, Geim A K, Morozov S V, Jiang D, Katsnelson M I, Grigorieva I V, Dubonos S V and Firsov A A 2005 Two-dimensional gas of massless Dirac fermions in graphene *Nature* **438** 197–200
- [2] Novoselov K S, Jiang D, Schedin F, Booth T J, Khotkevich V V, Morozov S V and Geim A K 2005 Two-dimensional atomic crystals *Proc. Natl. Acad. Sci. U. S. A.* **102** 10451–3
- [3] Pacilé D, Meyer J C, Girit Ç Ö and Zettl A 2008 The two-dimensional phase of boron nitride: Few-atomic-layer sheets and suspended membranes *Appl. Phys. Lett.* **92** 133107
- [4] Topsakal M, Aktürk E and Ciraci S 2009 First-principles study of two- and one-dimensional honeycomb structures of boron nitride *Phys. Rev. B* **79** 115442
- [5] König M, Wiedmann S, Brüne C, Roth A, Buhmann H, Molenkamp L W, Qi X-L and Zhang S-C 2007 Quantum Spin Hall Insulator State in HgTe Quantum Wells *Science* **318** 766–70
- [6] Cahangirov S, Topsakal M, Aktürk E, Şahin H and Ciraci S 2009 Two- and One-Dimensional Honeycomb Structures of Silicon and Germanium *Phys. Rev. Lett.* **102** 236804
- [7] Vogt P, De Padova P, Quaresima C, Avila J, Frantzeskakis E, Asensio M C, Resta A, Ealet B and Le Lay G 2012 Silicene: Compelling Experimental Evidence for Graphenelike Two-Dimensional Silicon *Phys. Rev. Lett.* **108** 155501
- [8] Dávila M E, Xian L, Cahangirov S, Rubio A and Lay G L 2014 Germanene: a novel two-dimensional germanium allotrope akin to graphene and silicene *New J. Phys.* **16** 095002
- [9] Özçelik V O, Durgun E and Ciraci S 2014 New Phases of Germanene *J. Phys. Chem. Lett.* **5** 2694–9
- [10] Tang P, Chen P, Cao W, Huang H, Cahangirov S, Xian L, Xu Y, Zhang S-C, Duan W and Rubio A 2014 Stable two-dimensional dumbbell stanene: A quantum spin Hall insulator *Phys. Rev. B* **90** 121408
- [11] Tao L, Cinquanta E, Chiappe D, Grazianetti C, Fanciulli M, Dubey M, Molle A and Akinwande D 2015 Silicene field-effect transistors operating at room temperature *Nat. Nanotechnol.* **10** 227–31
- [12] Wang Q H, Kalantar-Zadeh K, Kis A, Coleman J N and Strano M S 2012 Electronics and optoelectronics of two-dimensional transition metal dichalcogenides *Nat. Nanotechnol.* **7** 699–712

- [13] Chhowalla M, Shin H S, Eda G, Li L-J, Loh K P and Zhang H 2013 The chemistry of two-dimensional layered transition metal dichalcogenide nanosheets *Nat. Chem.* **5** 263–75
- [14] Jariwala D, Sangwan V K, Lauhon L J, Marks T J and Hersam M C 2014 Emerging Device Applications for Semiconducting Two-Dimensional Transition Metal Dichalcogenides *ACS Nano* **8** 1102–20
- [15] Xu X, Yao W, Xiao D and Heinz T F 2014 Spin and pseudospins in layered transition metal dichalcogenides *Nat. Phys.* **10** 343–50
- [16] Qian X, Liu J, Fu L and Li J 2014 Quantum spin Hall effect in two-dimensional transition metal dichalcogenides *Science* **346** 1344–7
- [17] Mak K F, Lee C, Hone J, Shan J and Heinz T F 2010 Atomically Thin  $\text{MoS}_2$ : A New Direct-Gap Semiconductor *Phys. Rev. Lett.* **105** 136805
- [18] Radisavljevic B, Radenovic A, Brivio J, Giacometti V and Kis A 2011 Single-layer  $\text{MoS}_2$  transistors *Nat. Nanotechnol.* **6** 147–50
- [19] Cong C, Shang J, Wu X, Cao B, Peimyoo N, Qiu C, Sun L and Yu T 2014 Synthesis and Optical Properties of Large-Area Single-Crystalline 2D Semiconductor  $\text{WS}_2$  Monolayer from Chemical Vapor Deposition *Adv. Opt. Mater.* **2** 131–6
- [20] Li L, Yu Y, Ye G J, Ge Q, Ou X, Wu H, Feng D, Chen X H and Zhang Y 2014 Black phosphorus field-effect transistors *Nat. Nanotechnol.* **9** 372–7
- [21] Novoselov K S, Geim A K, Morozov S V, Jiang D, Zhang Y, Dubonos S V, Grigorieva I V and Firsov A A 2004 Electric Field Effect in Atomically Thin Carbon Films *Science* **306** 666–9
- [22] Xia F, Wang H, Xiao D, Dubey M and Ramasubramaniam A 2014 Two-dimensional material nanophotonics *Nat. Photonics* **8** 899–907
- [23] Mas-Ballesté R, Gómez-Navarro C, Gómez-Herrero J and Zamora F 2011 2D materials: to graphene and beyond *Nanoscale* **3** 20–30
- [24] Butler S Z, Hollen S M, Cao L, Cui Y, Gupta J A, Gutiérrez H R, Heinz T F, Hong S S, Huang J, Ismach A F, Johnston-Halperin E, Kuno M, Plashnitsa V V, Robinson R D, Ruoff R S, Salahuddin S, Shan J, Shi L, Spencer M G, Terrones M, Windl W and Goldberger J E 2013 Progress, Challenges, and Opportunities in Two-Dimensional Materials Beyond Graphene *ACS Nano* **7** 2898–926
- [25] Geim A K and Grigorieva I V 2013 Van der Waals heterostructures *Nature* **499** 419–25
- [26] Nicolosi V, Chhowalla M, Kanatzidis M G, Strano M S and Coleman J N 2013 Liquid Exfoliation of Layered Materials *Science* **340** 1226419

- [27] Paton K R, Varrla E, Backes C, Smith R J, Khan U, O'Neill A, Boland C, Lotya M, Istrate O M, King P, Higgins T, Barwich S, May P, Puczarski P, Ahmed I, Moebius M, Pettersson H, Long E, Coelho J, O'Brien S E, McGuire E K, Sanchez B M, Duesberg G S, McEvoy N, Pennycook T J, Downing C, Crossley A, Nicolosi V and Coleman J N 2014 Scalable production of large quantities of defect-free few-layer graphene by shear exfoliation in liquids *Nat. Mater.* **13** 624–30
- [28] Oganov A R and Glass C W 2006 Crystal structure prediction using ab initio evolutionary techniques: Principles and applications *J. Chem. Phys.* **124** 244704
- [29] Oganov A R, Lyakhov A O and Valle M 2011 How Evolutionary Crystal Structure Prediction Works—and Why *Acc. Chem. Res.* **44** 227–37
- [30] Lyakhov A O, Oganov A R, Stokes H T and Zhu Q 2013 New developments in evolutionary structure prediction algorithm USPEX *Comput. Phys. Commun.* **184** 1172–82
- [31] Wang Y, Lv J, Zhu L and Ma Y 2012 CALYPSO: A method for crystal structure prediction *Comput. Phys. Commun.* **183** 2063–70
- [32] Li Y, Liao Y and Chen Z 2014 Be<sub>2</sub>C Monolayer with Quasi-Planar Hexacoordinate Carbons: A Global Minimum Structure *Angew. Chem. Int. Ed.* **53** 7248–52
- [33] Xiao H, Shi X, Hao F, Liao X, Zhang Y and Chen X 2016 Prediction of a Two-dimensional Sulfur Nitride (S<sub>3</sub>N<sub>2</sub>) Solid for Nanoscale Optoelectronic Applications *ArXiv160601597 Cond-Mat*
- [34] Perdew J P, Burke K and Ernzerhof M 1996 Generalized Gradient Approximation Made Simple *Phys. Rev. Lett.* **77** 3865–8
- [35] Segall M D, Lindan P J D, Probert M J, Pickard C J, Hasnip P J, Clark S J and Payne M C 2002 First-principles simulation: ideas, illustrations and the CASTEP code *J. Phys. Condens. Matter* **14** 2717
- [36] Payne M C, Teter M P, Allan D C, Arias T A and Joannopoulos J D 1992 Iterative minimization techniques for *ab initio* total-energy calculations: molecular dynamics and conjugate gradients *Rev. Mod. Phys.* **64** 1045–97
- [37] Monkhorst H J and Pack J D 1976 Special points for Brillouin-zone integrations *Phys. Rev. B* **13** 5188–92
- [38] Grimme S 2006 Semiempirical GGA-type density functional constructed with a long-range dispersion correction *J. Comput. Chem.* **27** 1787–99
- [39] Sham L J and Schlüter M 1983 Density-Functional Theory of the Energy Gap *Phys. Rev. Lett.* **51** 1888–91
- [40] Perdew J P and Levy M 1983 Physical Content of the Exact Kohn-Sham Orbital Energies: Band Gaps and Derivative Discontinuities *Phys. Rev. Lett.* **51** 1884–7

- [41] Hedin L 1965 New Method for Calculating the One-Particle Green's Function with Application to the Electron-Gas Problem *Phys. Rev.* **139** A796–823
- [42] Marini A, Hogan C, Grüning M and Varsano D 2009 yambo: An ab initio tool for excited state calculations *Comput. Phys. Commun.* **180** 1392–403
- [43] Giannozzi P, Baroni S, Bonini N, Calandra M, Car R, Cavazzoni C, Davide Ceresoli, Chiarotti G L, Cococcioni M, Dabo I, Corso A D, Gironcoli S de, Fabris S, Fratesi G, Gebauer R, Gerstmann U, Gougoussis C, Anton Kokalj, Lazzeri M, Martin-Samos L, Marzari N, Mauri F, Mazzarello R, Stefano Paolini, Pasquarello A, Paulatto L, Sbraccia C, Scandolo S, Sclauzero G, Seitsonen A P, Smogunov A, Umari P and Wentzcovitch R M 2009 QUANTUM ESPRESSO: a modular and open-source software project for quantum simulations of materials *J. Phys. Condens. Matter* **21** 395502
- [44] Aulbur W G, Jönsson L and Wilkins J W 2000 Quasiparticle Calculations in Solids *Solid State Physics* vol 54, ed H E and F Spaepen (Academic Press) pp 1–218
- [45] VandeVondele J and Hutter J 2007 Gaussian basis sets for accurate calculations on molecular systems in gas and condensed phases *J. Chem. Phys.* **127** 114105
- [46] VandeVondele J, Krack M, Mohamed F, Parrinello M, Chassaing T and Hutter J 2005 Quickstep: Fast and accurate density functional calculations using a mixed Gaussian and plane waves approach *Comput. Phys. Commun.* **167** 103–28
- [47] Zandiatashbar A, Lee G-H, An S J, Lee S, Mathew N, Terrones M, Hayashi T, Picu C R, Hone J and Koratkar N 2014 Effect of defects on the intrinsic strength and stiffness of graphene *Nat. Commun.* **5** 3186
- [48] Wang G, Slough W J, Pandey R and Karna S P 2016 Degradation of phosphorene in air: understanding at atomic level *2D Mater.* **3** 025011